



# Exploring Building Materials with Raman Spectroscopy:

## A Beginner's Journey through Research Progress and Discoveries

Wednesday 10 am, Sep 13, 2023, Room 421, Blgd 35



**Presented by Jiseul Park**  
Postdoctoral Researcher



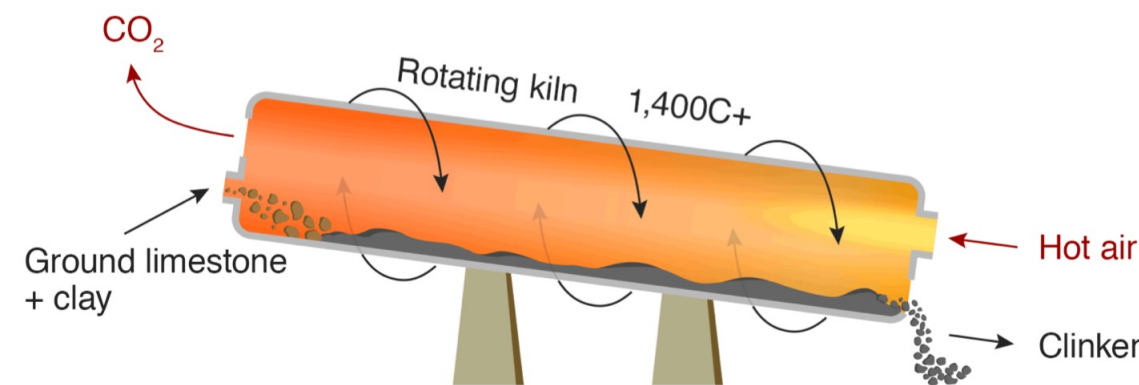
**Multiscale Structural Materials Lab.**  
Advanced Technology in Structural Materials

# Contents

1. Introduction
2. Fundamentals of Raman microspectroscopy
3. Processing Raman data
4. Applications in Building Materials
5. Conclusion

# Concrete and cement

- Concrete: the most widely used, durable, versatile, and strong construction material over 100 yrs
- Cement (binder) + gravel + sand + water
- Ordinary Portland cement (OPC): Calcium silicate based, hydraulic material
- Production of 1 ton of cement emits 0.9 ton of CO<sub>2</sub>



# Low carbon concrete/cement

- Replace cement clinker by limestone and calcined clay (LC3)
- Utilization of industrial byproduct: slags from iron making process, ashes from power plants
- Mineral carbonation by injecting CO<sub>2</sub> into concrete (carbon utilization/storage)
- **Before we use this low carbon product to construction site**
  - The characterisation of microstructure is an important step towards understanding durability mechanisms in cementitious materials
  - But it is always getting more challenging due to multi-scale hierarchy, multi-phases – crystalline and amorphous, heterogeneous characteristic, phase evolution with time, ...

# We use multiple techniques to study cementitious system

Qualitive and quantitative analysis of crystalline phases

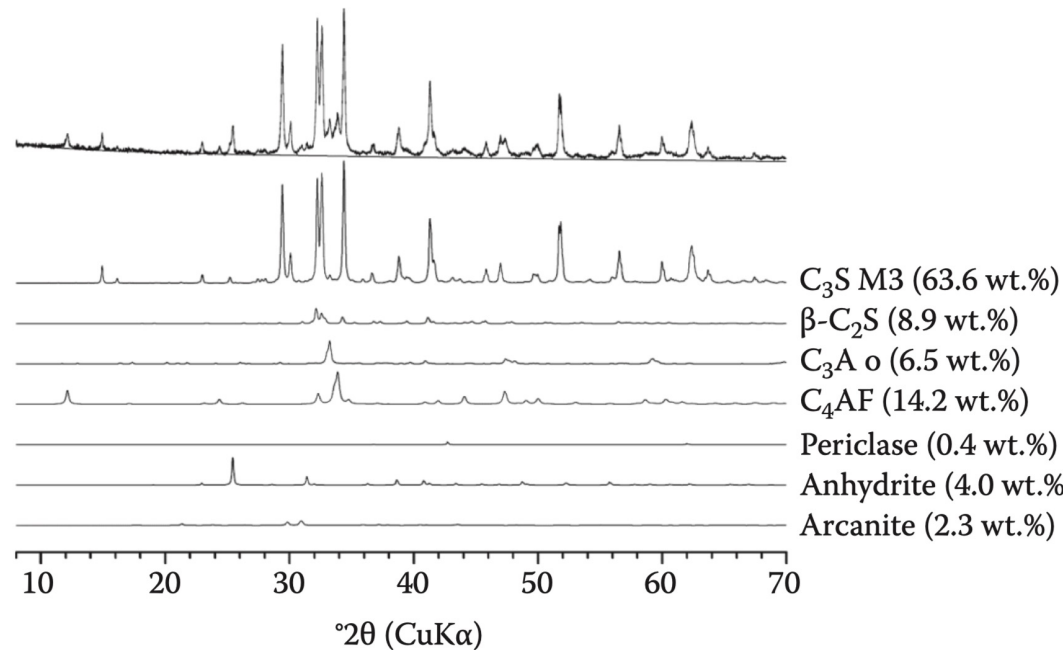


Figure. XRD scan of a portland cement (CEM I 52.5 N) (top) and its pattern decomposition calculated by Rietveld QPA (Scrivener et al., 2018)

- **X-ray diffraction(XRD)/Rietveld method**

: to identify and quantify the different crystalline in the cement and their hydration products, and the amount of amorphous phases

# We use multiple techniques to study cementitious system

Complementary information for XRD data

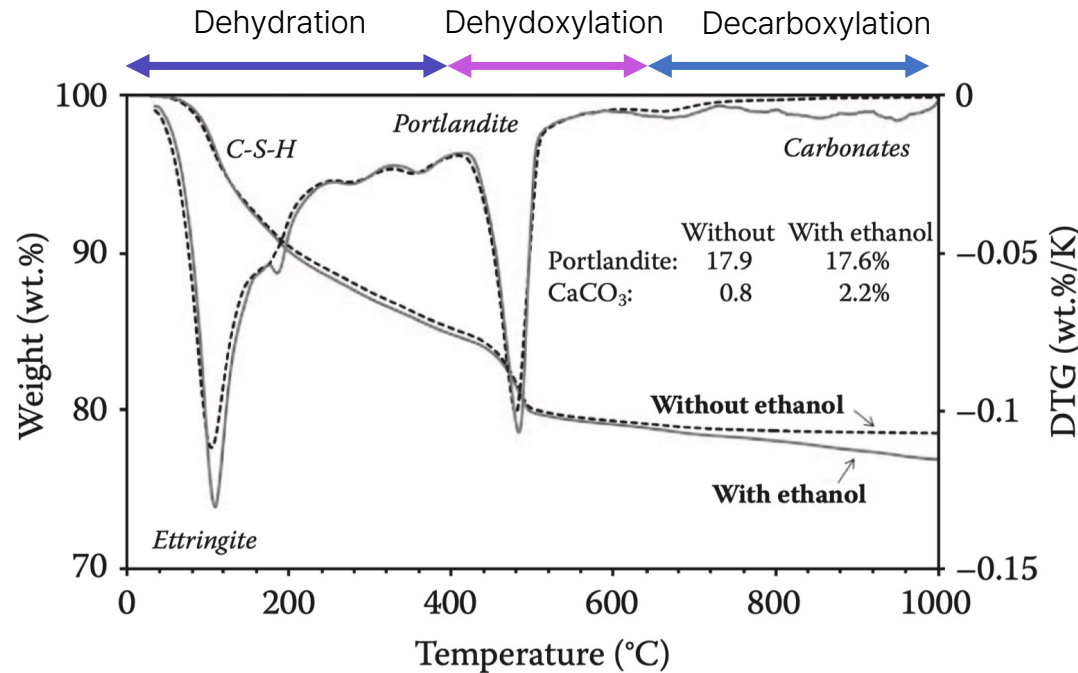
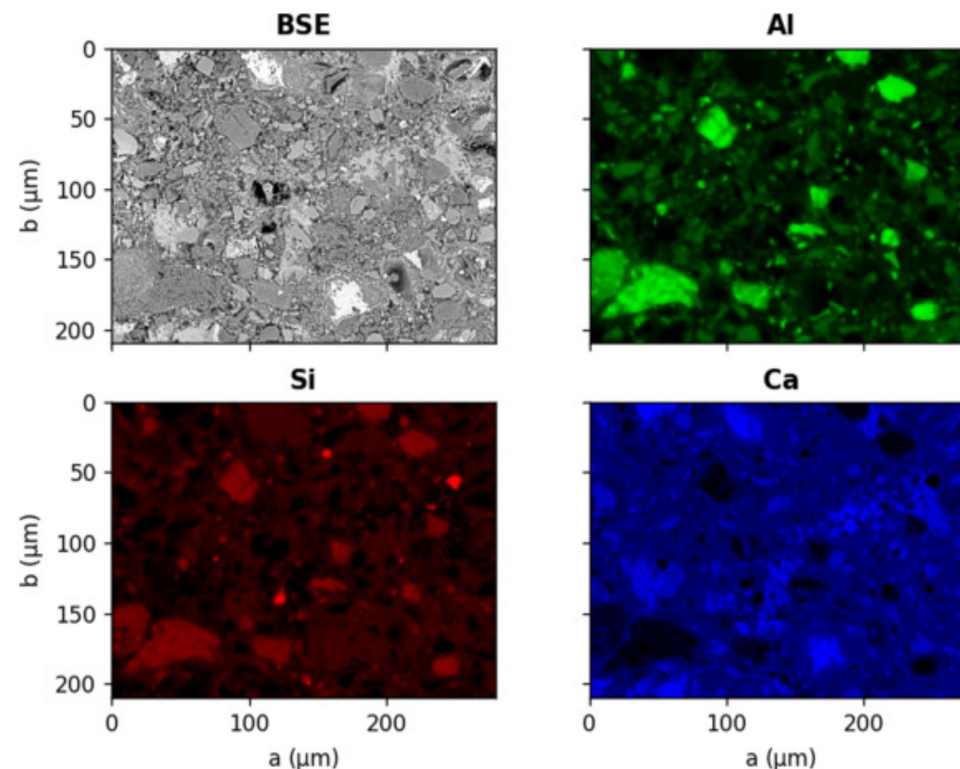


Figure. TGA and DTG curves for a 91-day-hydrated ordinary portland cement (De Weerdt et al. 2011).

- **Thermogravimetric(TG) analysis**  
: to confirm the XRD data and to characterize the main amorphous phases

# We use multiple techniques to study cementitious system

Spatial distribution and composition of elements



- Scanning electron microscope/energy dispersive spectrometer (SEM-EDS)  
: to assess the chemical composition of phases in cementitious paste

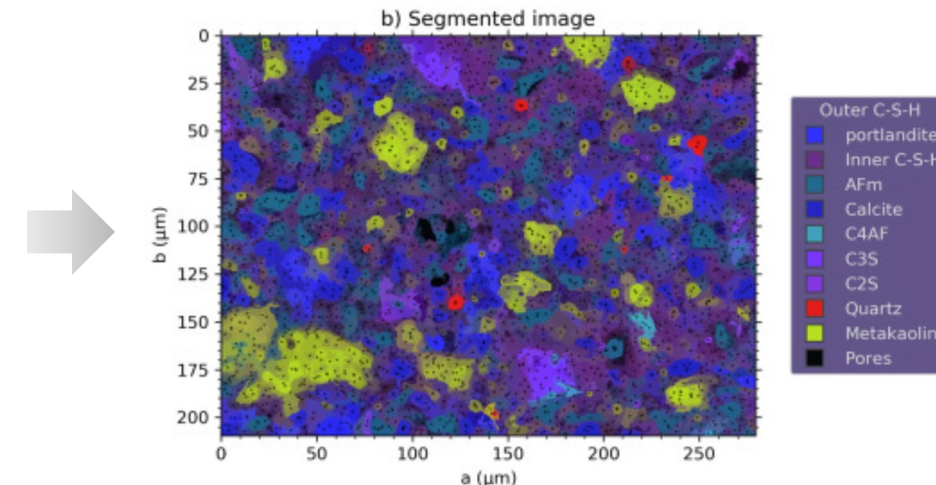


Figure. (Left) Components of a composite image and (Right) segmentation from composite image formed from the combination of the individual channels (Georget et al., 2021).

# Limitations of conventional techniques

- **Destructive, time consuming sample preparation**
  - Crush hardened solid specimen to *powder*
  - *Hydration stoppage* (remove water) at each age by solvent exchange
- **SEM-EDS**; Elemental map *cannot be directly used* for phase identification
- **XRD**; *Limited to crystalline phase*
- **TG**; In complex system, only the weight loss of H<sub>2</sub>O and CO<sub>2</sub> can be distinguished,  
*but not possible to distinguish from which phase the weight loss occurred*

# Potential of Raman microspectroscopy

- When we need imaging of hydration/carbonation *in-situ* (NO sample preparation) and *operando* (reflecting real-world conditions)
- When we need the time-spatial-resolved information to answer to these kinds of quenstions:
  - **Where** does strätlingite (hydrate product) precipitate **when** it forms?
  - Does exposure to chlorides change **the morphology** of AFm phases?
  - What is the impact of sulfates on **the hydration process**?

Raman microspectroscopy is an excellent candidate!

Why?

# Potential of Raman microspectroscopy

- Greatest strength of Raman spectroscopy is **flexible sampling**
  - powders, slurries, pellets, fibers, emulsions, or films, can be analyzed
- A single Raman spectrum can provide **a large amount of information**
  - **Qualitative and quantitative** analysis is possible
- **Common matrix** or container materials, such as water, pharmaceutical excipients, glass, and catalyst supports, have **weak Raman spectra**
  - therefore matrix/container materials generate relatively **little interference during analyte determination**

# Raman scattering

Laser beam > Molecule vibration (or rotation, electronic transition)

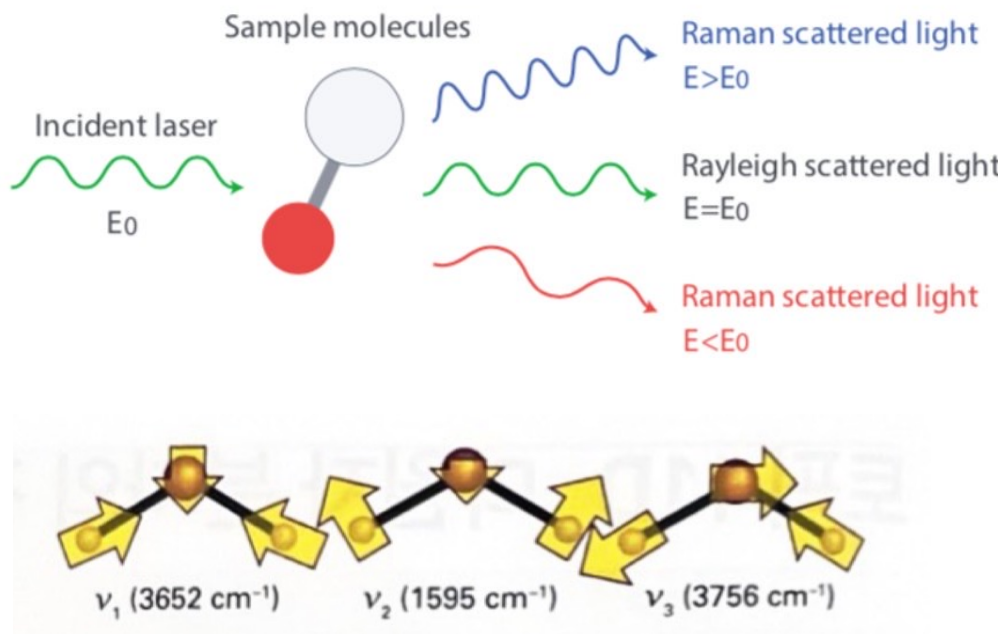


Figure. Vibrational modes of water molecule

$$E = E_0 \cos 2\pi\nu_0 t,$$

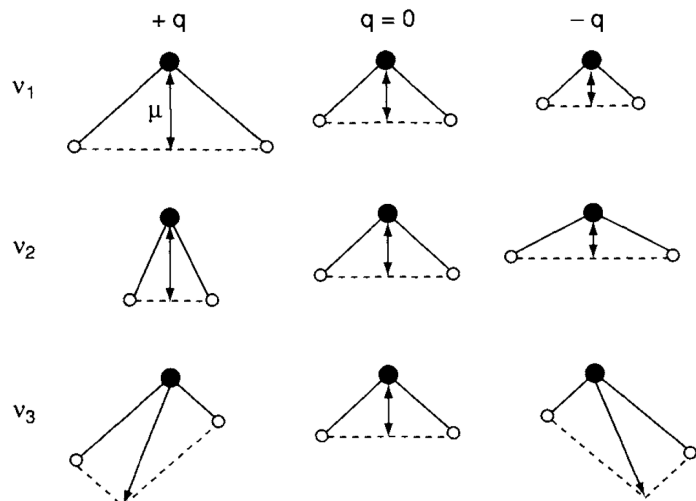
- $E$ : Electrical field strength of laser beam
- $\nu_0$ : frequency of laser beam

\* The unit of frequency is  $\text{cm}^{-1}$

- $\text{cm}^{-1}$ : a unit of frequency, wavenumber, the number of wave in unit distance (i.e., 1 cm)
- e.g., Light with a wavelength of 500 nm (green) has a wavenumber of  $20,000 \text{ cm}^{-1}$

# Raman scattering

Laser beam > Molecule vibration > Dipole moment > Radiation of light (Rayleigh, Raman scattering)

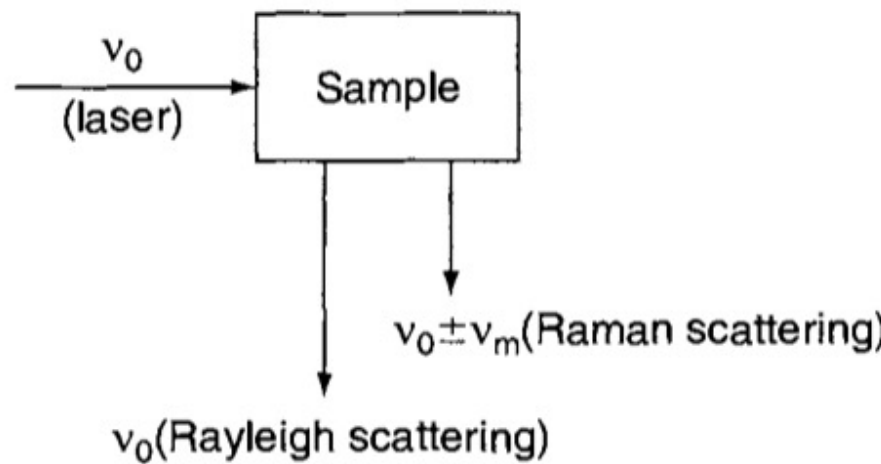


$$\begin{aligned}
 P &= \alpha E = \alpha_0 E_0 \cos 2\pi\nu_0 t. && \text{Rayleigh scattering; same frequency} \\
 &= \alpha_0 E_0 \cos 2\pi\nu_0 t + \frac{1}{2} \left( \frac{\partial \alpha}{\partial q} \right)_0 q_0 E_0 [ \cos \{2\pi(\nu_0 + \nu_m)t\} + \cos \{2\pi(\nu_0 - \nu_m)t\} ] && \text{Raman scattering; frequency changed} \\
 \alpha &= \alpha_0 + \left( \frac{\partial \alpha}{\partial q} \right)_0 q_0 + \dots && \\
 q &= q_0 \cos 2\pi\nu_m t, && \\
 \end{aligned}$$

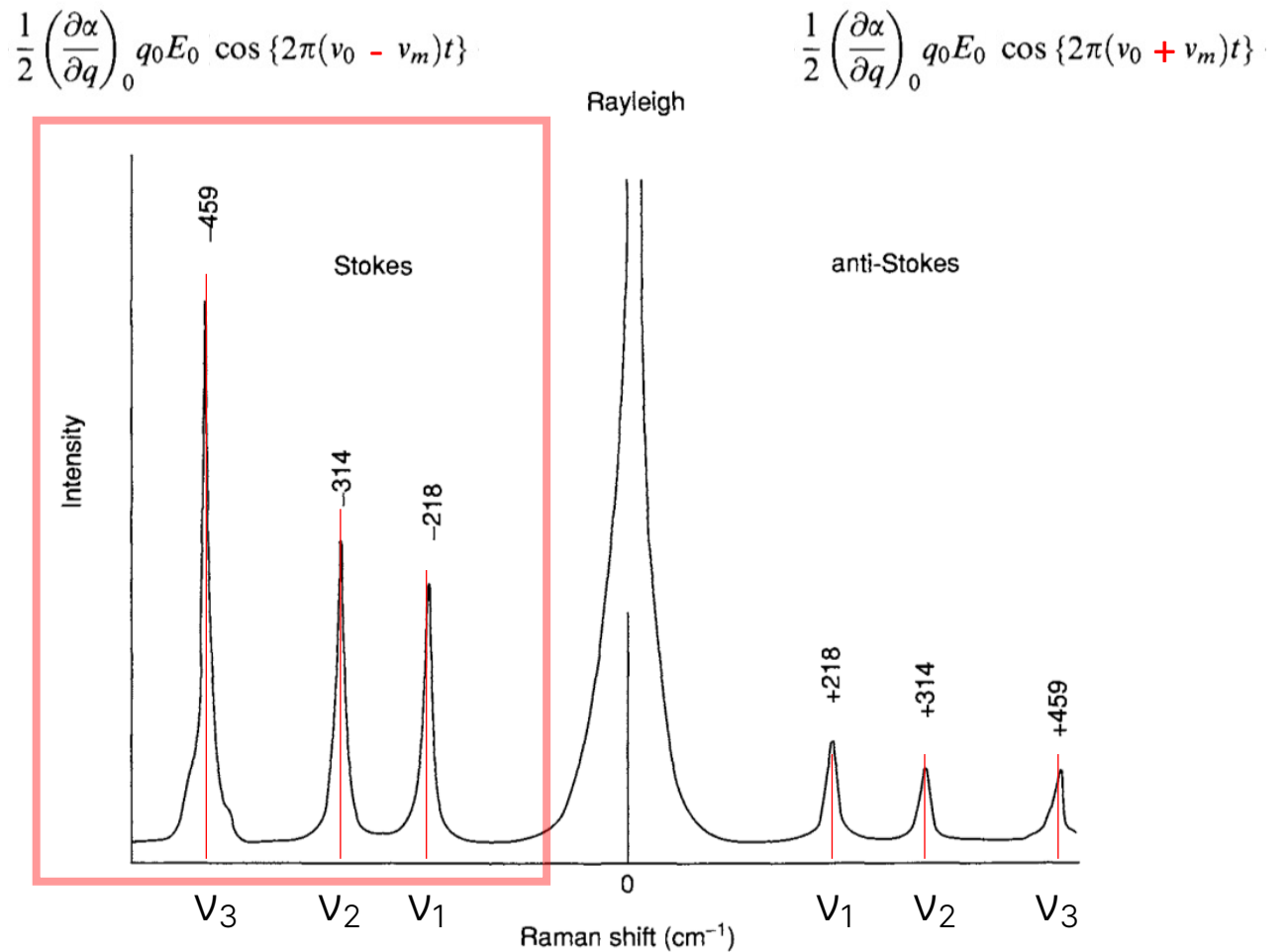
- $P$ : electric dipol moment induced
- $\alpha$ : polarizability
- the rate of change of  $\alpha$  w.r.t the change in  $q$
- $q$ : the nuclear displacement
- $\nu_m$  : vibrational frequency of a molecule

Figure. Change in dipole moment of water molecule during each normal vibration

# Raman spectrum



- The Stokes lines are stronger than the anti-Stokes lines under normal conditions
- It is common to measure only the Stokes side of the spectrum

Figure. Raman spectrum of  $\text{CCl}_4$  (488 nm excitation)

# How many Raman peaks would we expect?

- **Example for the analysis of vibrational modes of water molecule**  
(\* pre-requisite: Group theory, the symmetry of point/space group)

1. Calculate the degree of freedom of the molecule vibration
  - Linear Molecule Degrees of Freedom =  $3N-5$
  - Non-Linear Molecule Degrees of Freedom =  $3N-6$

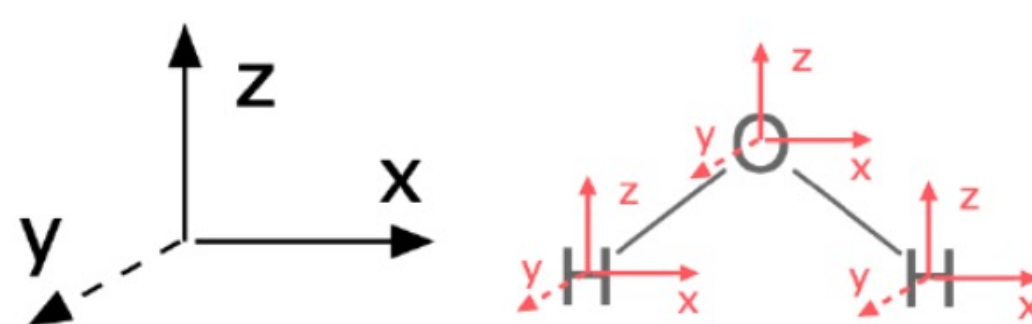


Figure. The first step to finding normal modes is to assign a consistent axis system to the entire molecule and to each atom (Kathryn Haas).

# How many Raman peaks would we expect?

2. Find the point group of the molecule

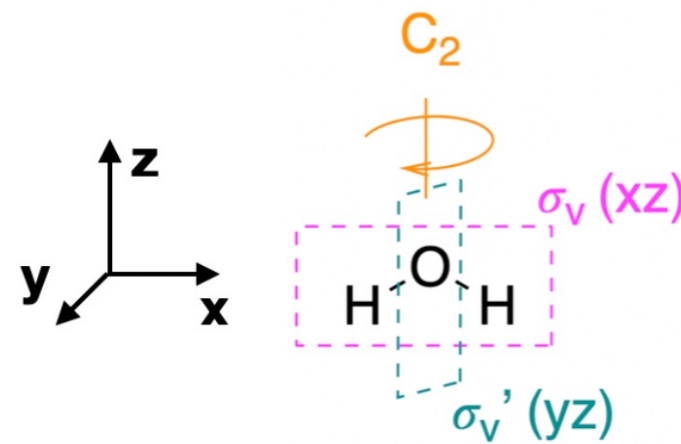


Figure. The water molecular is in the  $C_{2v}$  point group (Kathryn Haas).

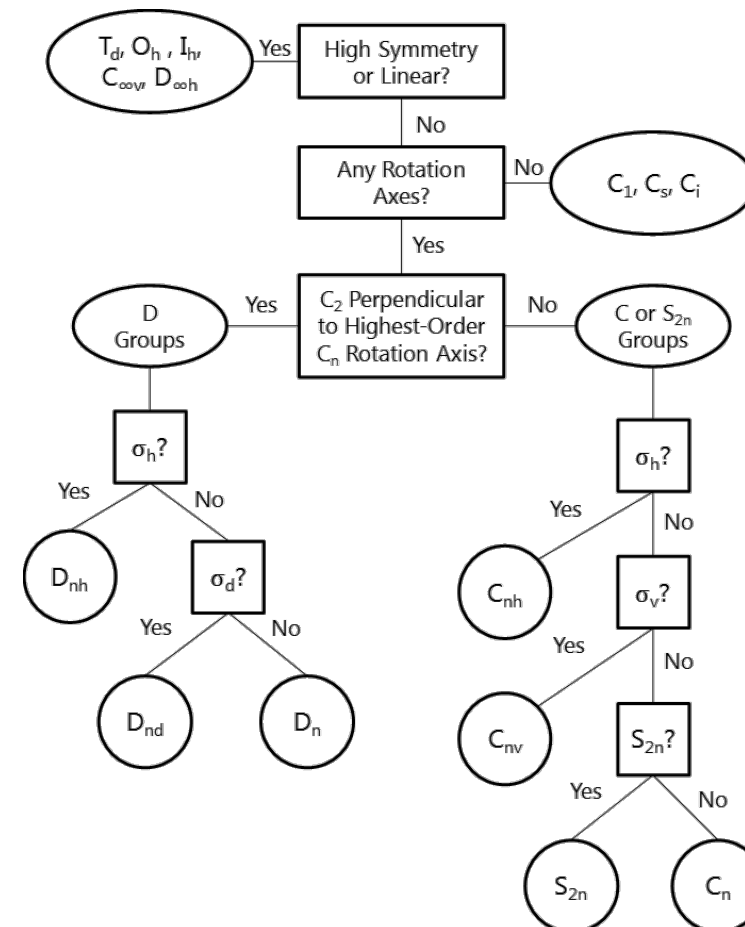


Figure. Flow chart for point group assignment.

# How many Raman peaks would we expect?

3. Find the reducible representation for all normal modes

- Use the C<sub>2v</sub> character table to generate one reducible representation ( $\Gamma$ )

$C_{2v}$	$E$	$C_2$	$\sigma_v$	$\sigma'_v$
$\Gamma_{modes}$	9	-1	3	1

4. Break normal modes into irreducible representation

$$\Gamma_{modes} = 3A_1 + 1A_2 + 3B_1 + 2B_2$$

# How many Raman peaks would we expect?

5. Subtract rotations and translations to find vibrational modes

$$\begin{aligned}
 H_2O \text{ vibrations} &= \Gamma_{modes} - \text{Rotations} - \text{Translations} \\
 &= (3A_1 + 1A_2 + 3B_1 + 2B_2) - (A_1 - B_1 - B_2) - (A_2 - B_1 - B_2) \\
 &= 2A_1 + 1B_1
 \end{aligned}$$

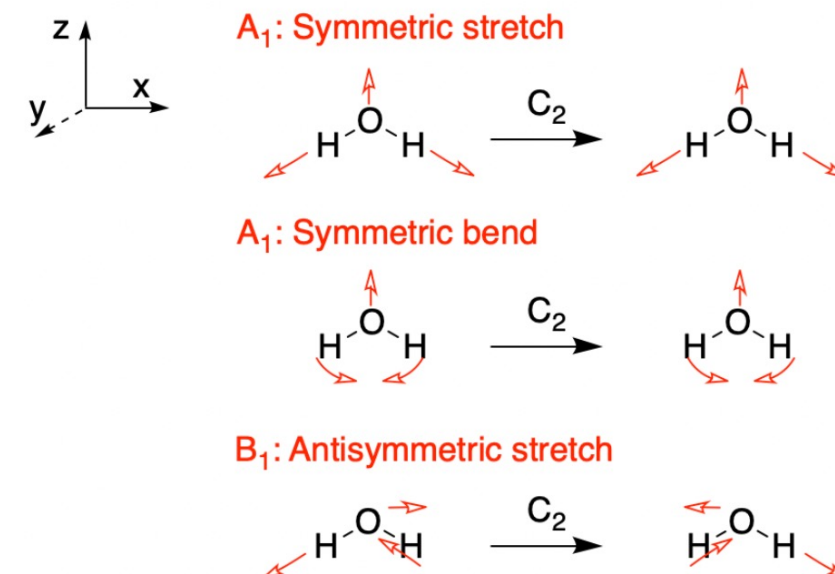


Figure. Illustration of the vibrational motions of water (Kathryn Haas).

# How many Raman peaks would we expect?

## 5. Subtract rotations and translations to find vibrational modes

- If a vibration results in a change in the molecular polarizability, it is Raman-active.
- In the character table, we can recognize the vibrational modes that are Raman-active by those with symmetry of any of the binary products ( $xy$ ,  $xz$ ,  $yz$ ,  $x^2$ ,  $y^2$ , and  $z^2$ ) or a linear combination of binary products (e.g.  $x^2-y^2$ ).

Table. The C<sub>2v</sub> character table

$C_{2v}$	$E$	$C_2$	$\sigma_v$	$\sigma'_v$	$h = 4$	
$A_1$	1	1	1	1	$z$	$x^2, y^2, z^2$
$A_2$	1	1	-1	-1	$R_z$	$xy$
$B_1$	1	-1	1	-1	$x, R_y$	$xz$
$B_2$	1	-1	-1	1	$y, R_x$	$yz$

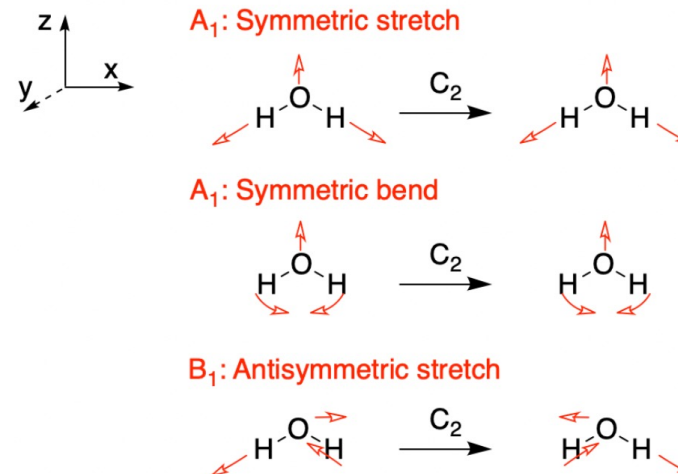


Figure. Illustration of the vibrational motions of water (Kathryn Haas).

# Raman peak profile: intensity, width, and position

- **Raman peak intensity**

- proportional to the intensity & frequency of the laser and the number of molecules in the interaction volume (→ mole fraction),
- and is a result of molecular vibration causing a change in polarizability rate of the molecule (→ Raman sensitivity, Raman cross-section)

$$I(\nu) = \frac{2^4 \pi^3}{45 \cdot 3^2 \cdot c^4} \cdot \frac{h I_L N (\nu_0 - \nu)^4}{\mu \nu (1 - e^{-h\nu/kT})} \times [45(\alpha_a')^2 + 7(\gamma_a')^2] = C \cdot I_0 \cdot n \cdot \sigma$$

- The sensitivity of equipment can be increased using a stronger laser (488 nm > 532 nm > 785 nm)
- **The proportional relationship** between Raman scattering **intensity and analyte concentration** is the basis for the quantitative Raman analysis

# Raman peak profile: intensity, width, and position

- Raman peak width
  - Related to crystallinity and homogeneity
  - e.g., calcium hydroxide (CH) is well crystalline hydrate phase.
  - However, in early-age hydration disordered CH (DCH) is formed and identified with peak broadening

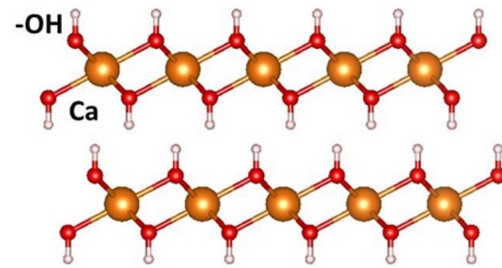


Figure. Crystal structure of calcium hydroxide.

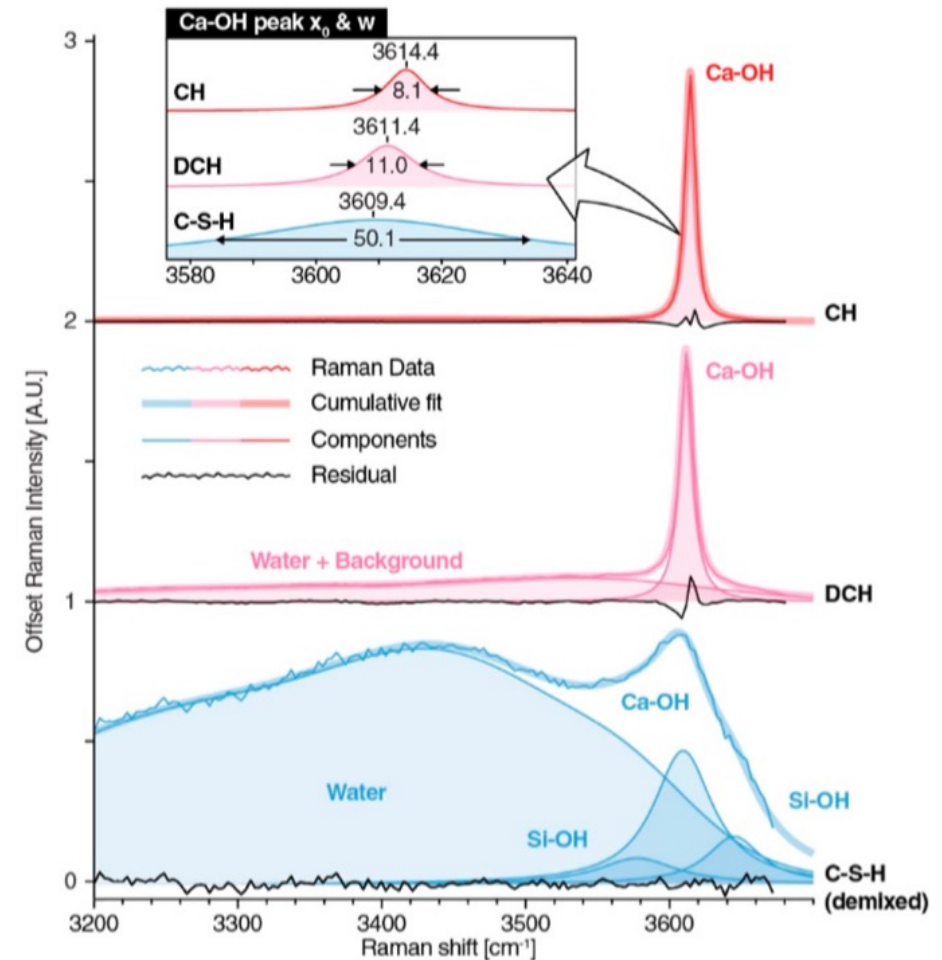


Figure. Raman spectra of CH, DCH, and C-S-H (Loh et al, 2021).

# Raman peak profile: intensity, width, and position

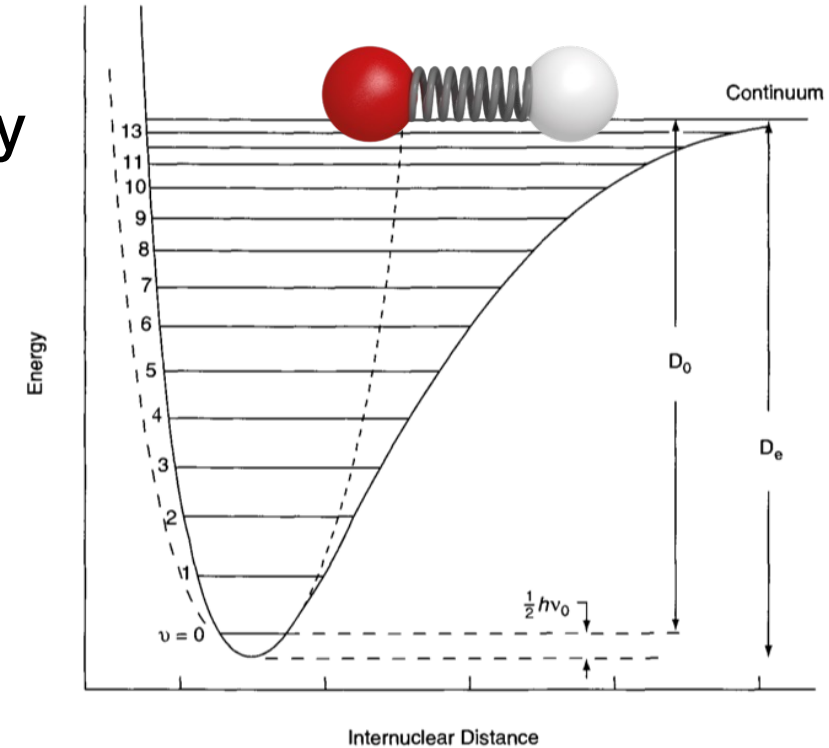
- Raman peak position = vibrational frequency
  - When the chemical bond between two atoms is regarded as a spring

$$\nu_0 = \frac{1}{2\pi} \sqrt{\frac{K}{\mu}}.$$

Force constant  
Mass

$$K = \left( \frac{d^2 V}{dq^2} \right)_{q \rightarrow 0}$$

The curvature of the potential well near the equilibrium position



- A **force constant** is the curvature of the potential well near the equilibrium position
- Therefore, a large force constant does not necessarily mean a stronger bond...
- \* The bond strength is measured by the depth of the potential wall

# Raman peak profile: intensity, width, and position

- Raman peak position**

- Related to vibrational frequency, therefore can be altered by different chemical and mechanical environments, such as pH, temperature, and stress.
- e.g., ettringite and monosulfoaluminate (hydrate products of aluminate)

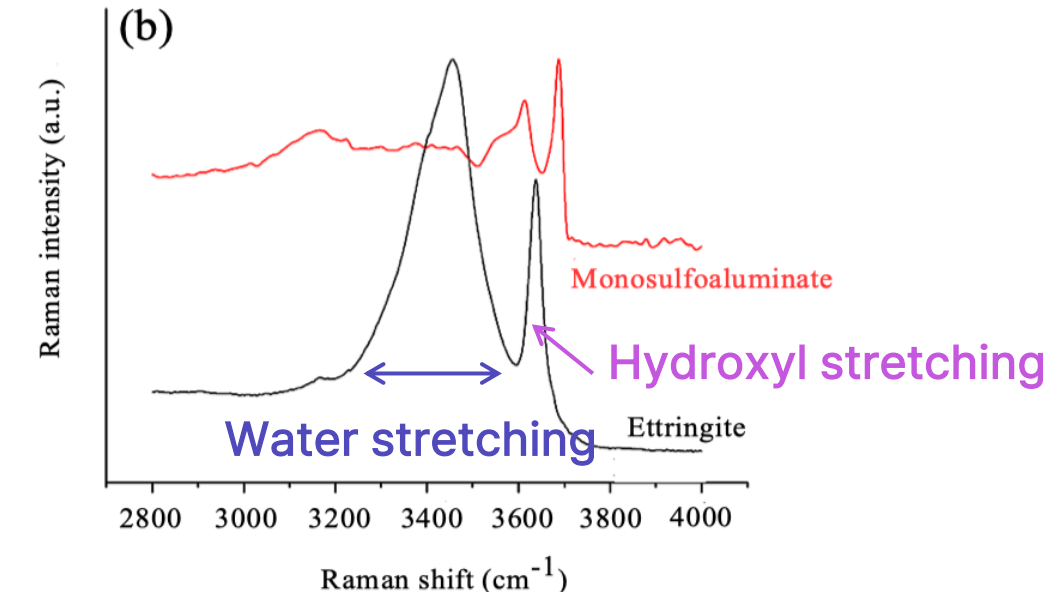
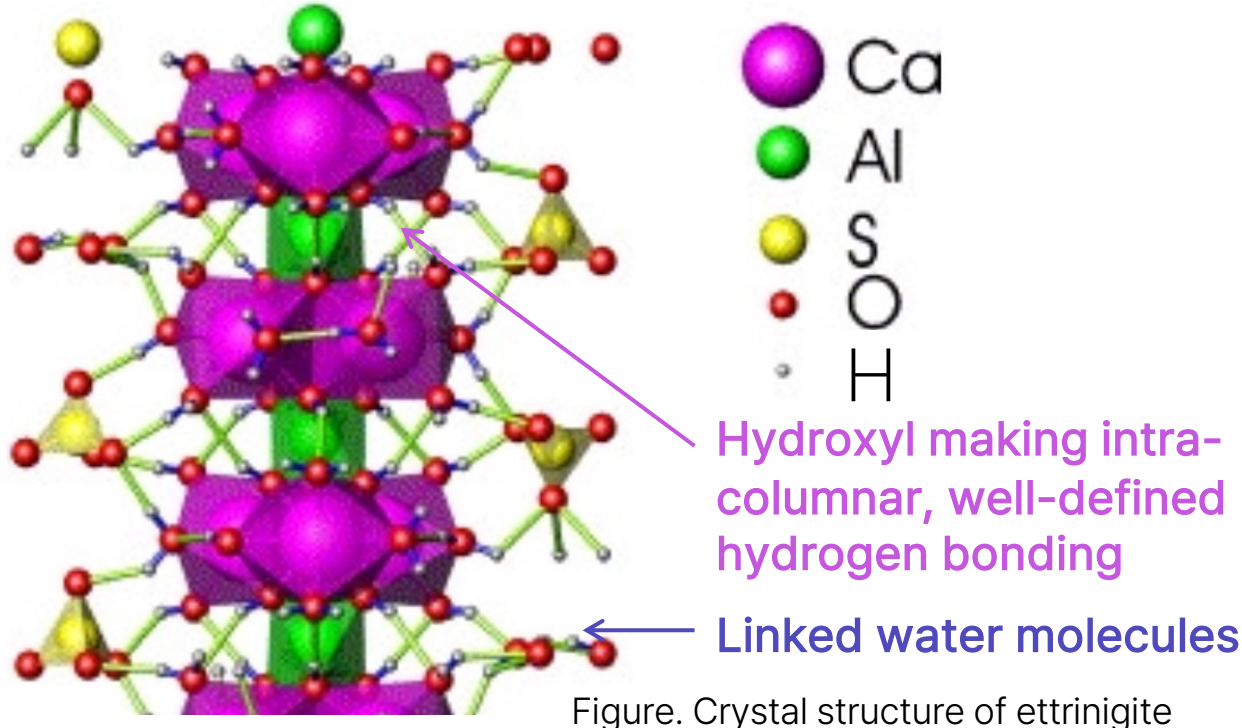


Figure. Raman spectra of synthesized ettringite and monosulfoaluminate (Renaudin et al, 2007)

# Raman peak profile: intensity, width, and position

- Raman peak position**

- Related to vibrational frequency, therefore can be altered by different chemical and mechanical environments, such as pH, temperature, and stress.
- e.g., ettringite and monosulfoaluminate (hydrate products of aluminate)

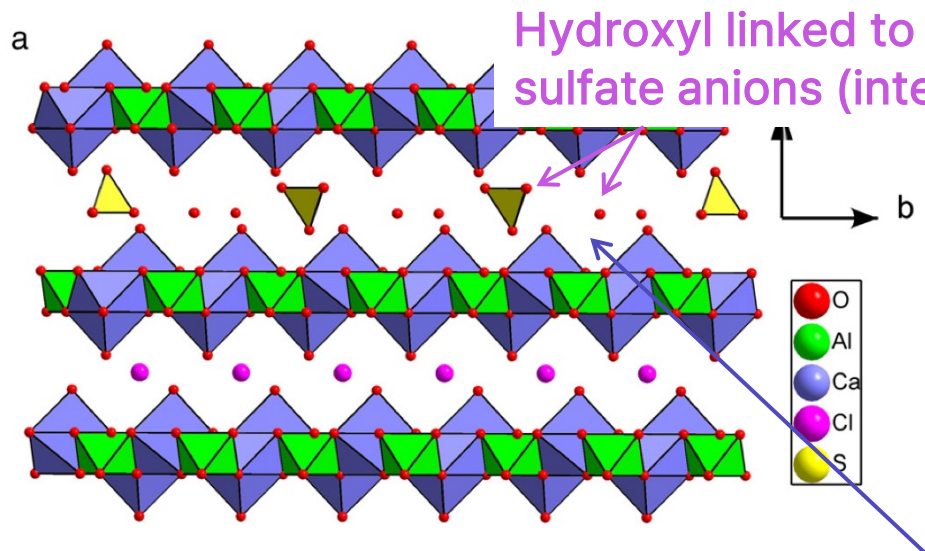
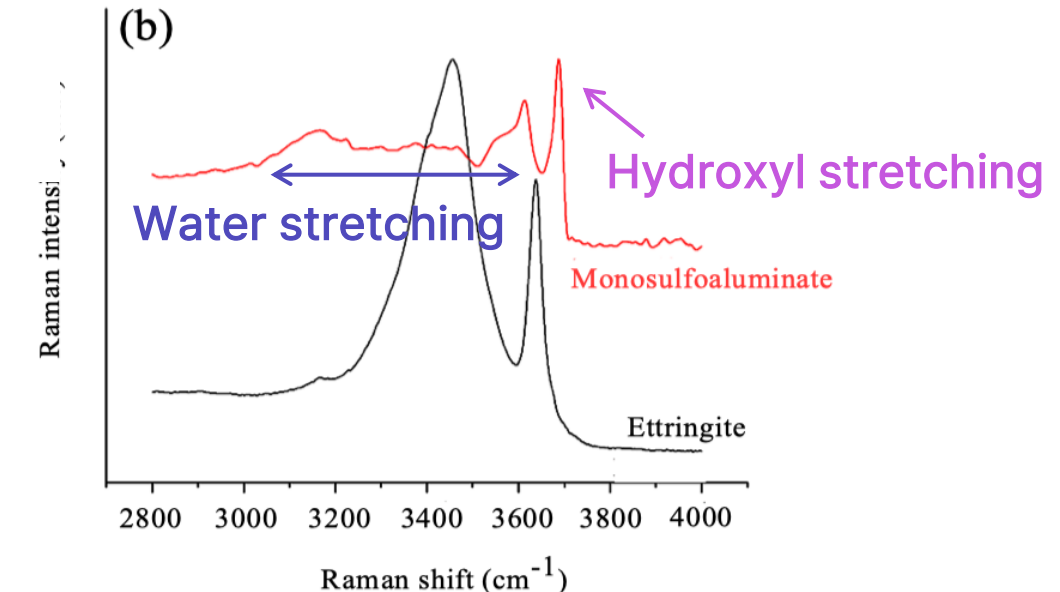


Figure. Crystal structure of monosulfoaluminate



- 1) statistical occupancy disorder
- 2) orientation disorder of sulfate tetrahedron in the interlayer

# Raman peak profile: intensity, width, and position

- **Raman peak position**
  - Is sensitive to the interatomic forces, depending on small changes in bond length and bond angles
  - e.g., **laser-induced sample heating**

→ Peak frequencies shift toward lower wavenumbers due to **bond length expansion with sample heating**

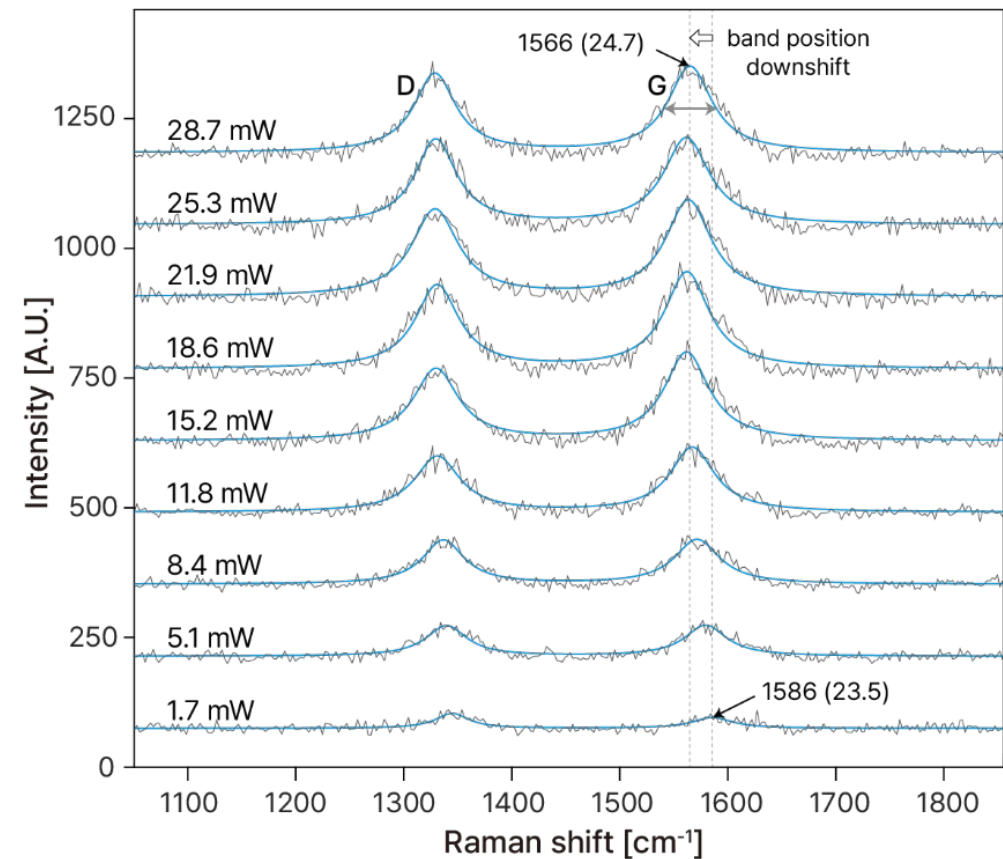


Figure. Raman spectra of multi-walled CNT powders with varying laser power levels.

# Processing Raman spectra

## Typical processing flow of Raman spectra in building materials

### Preprocessing



- Cosmic ray removal
- Baseline correction
- Signal-to-noise calculation

### Basis analysis



- De-mixing
- Assignment of Raman peaks to each vibrational mode

### Phase map construction



- Curve fitting to the superposition of basis spectra

### Peak analysis

- Curve fitting to the Gaussian or Lorentzian function

# Cosmic ray removal

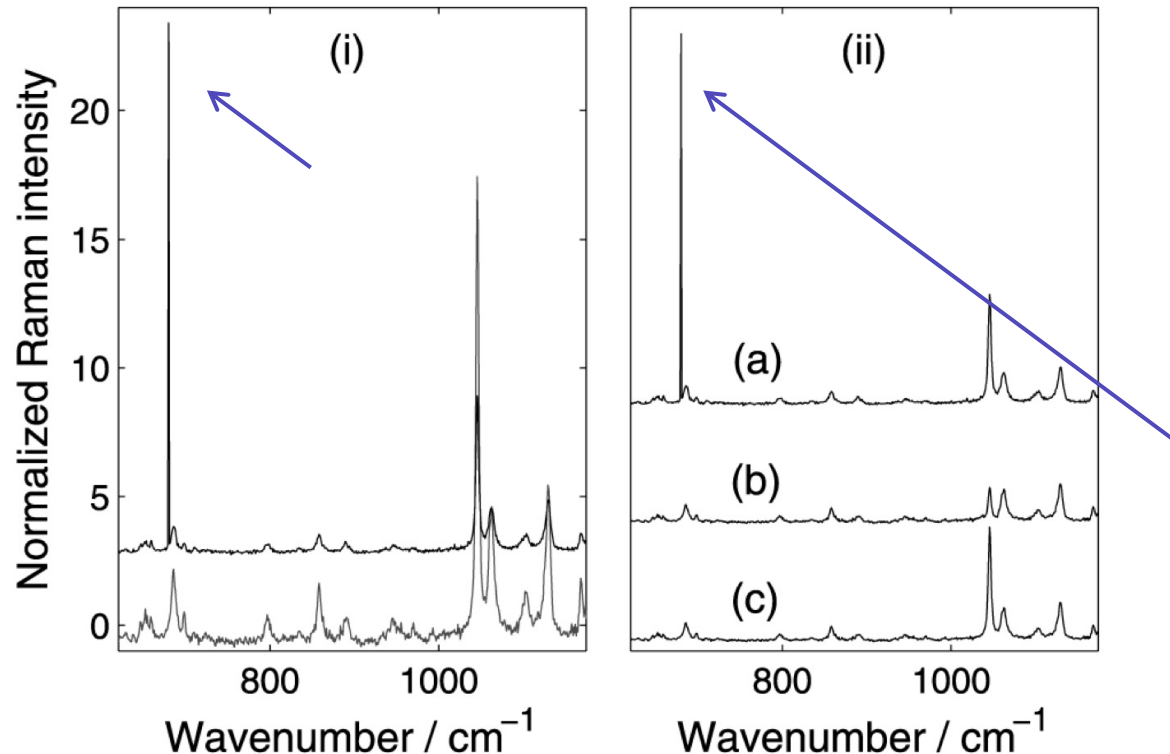
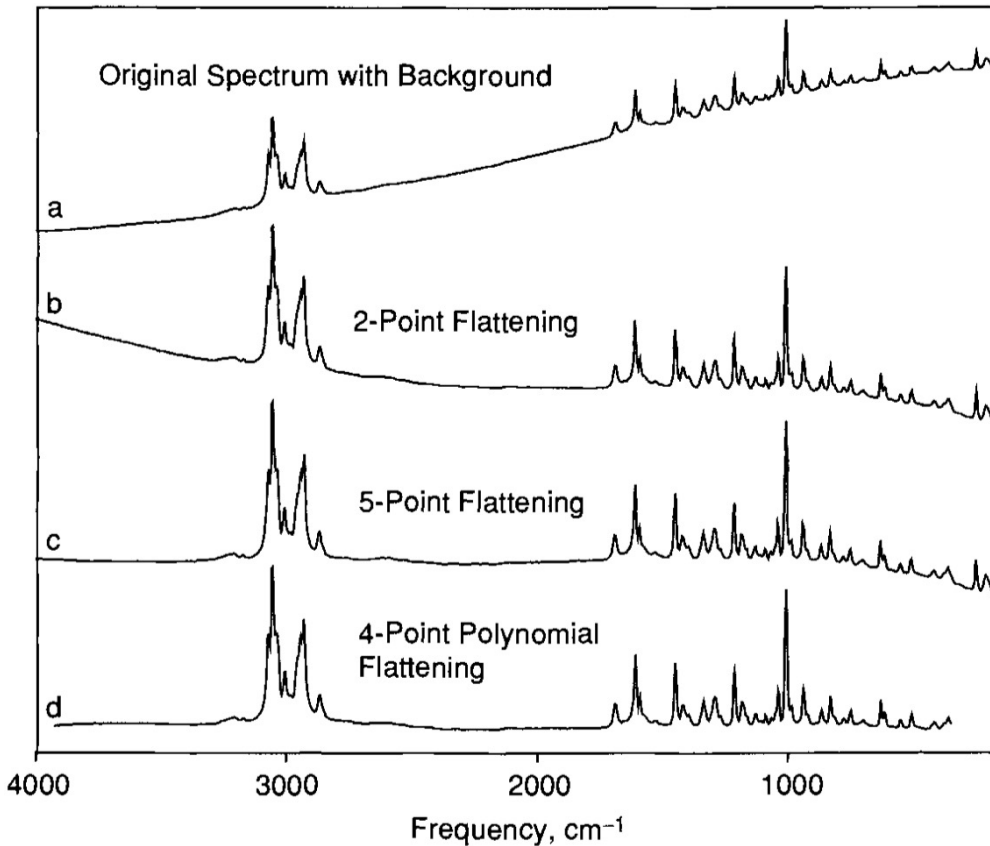


Figure. Examples of cosmic ray in Raman spectra  
(Cappel et al., 2001).

- intensity spikes created when high-energy particles such as cosmic rays pass through the detector of the Raman instrument
- the effected points in the Raman spectrum can be replaced by estimates of what the intensity should have been by averaging for example

# Baseline correction



- sometimes the baseline is a few orders more intense as compared with Raman-bands
- lots of algorithms has been suggested
  - Derivative calculation
  - Polynomial fitting
  - Sensitive nonlinear iterative peak (SNIP) clipping
  - Asymmetric least squares (ALS)
- Important information may be lost and important spectral bands may be distorted

Figure. The effect of different baseline flattening routines: (2) original spectrum; (b) two-point linear fit of baseline; (c) five-point linear fit of baseline; (d) four-point polynomial ft of baseline ( ).

# Basis analysis

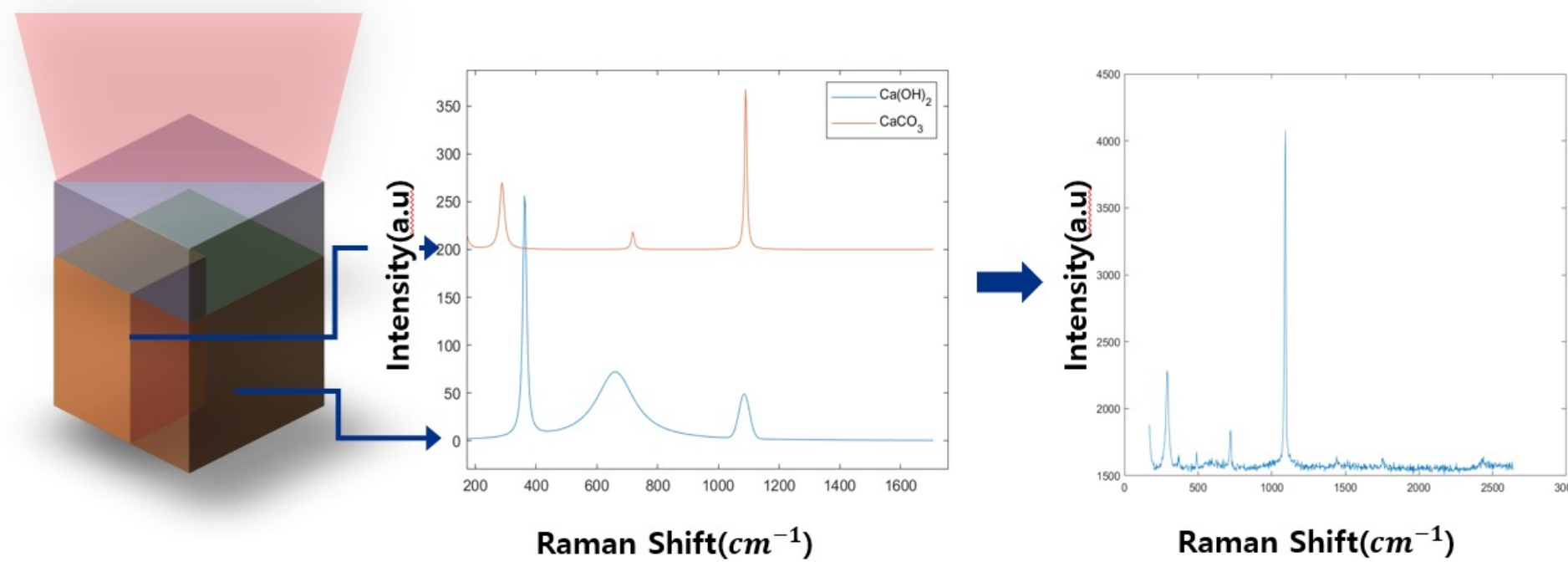


Figure. Graphical representation of laser spot acquiring heterogeneous material.  
Heterogeneous system may contain more than single material in a laser spot (Lee., 2023).

# Manual clustering and profile fitting is possible..

- You can build your own library for peak assignment of each phase referring to previous studies, open database (e.g., RRUFF)
- Then, clustering spectra using algorithms such as Self-organizing map (SOM)
- Profile fitting using Gaussian or Lorentzian function
- De-mixing the spectra of mixture

**Table 1. Raman Peak Assignment of C–S–H<sup>a</sup>**

Vib. modes	This study	Previous studies
Ca–O LV	337 <sub>m</sub>	310–360
Si–O–Si SB	Q <sub>3</sub> N/A Q <sub>2</sub> Q <sub>1</sub>	600–630 660 <sub>m</sub> 675 858 <sub>w</sub> , 897 <sub>w</sub>
SiO <sub>4</sub> SS	Q <sub>1</sub> Q <sub>2</sub> Q <sub>3</sub>	860–900 983 <sub>m</sub> 1064 <sub>w</sub>
OH SS	H <sub>2</sub> O Ca–OH Si–OH	3245–3600 3609 <sub>s</sub> 3578 <sub>sh</sub> , 3645 <sub>sh</sub>

<sup>a</sup>s: strong, m: medium, w: weak, sh: shoulder, b: broadened.

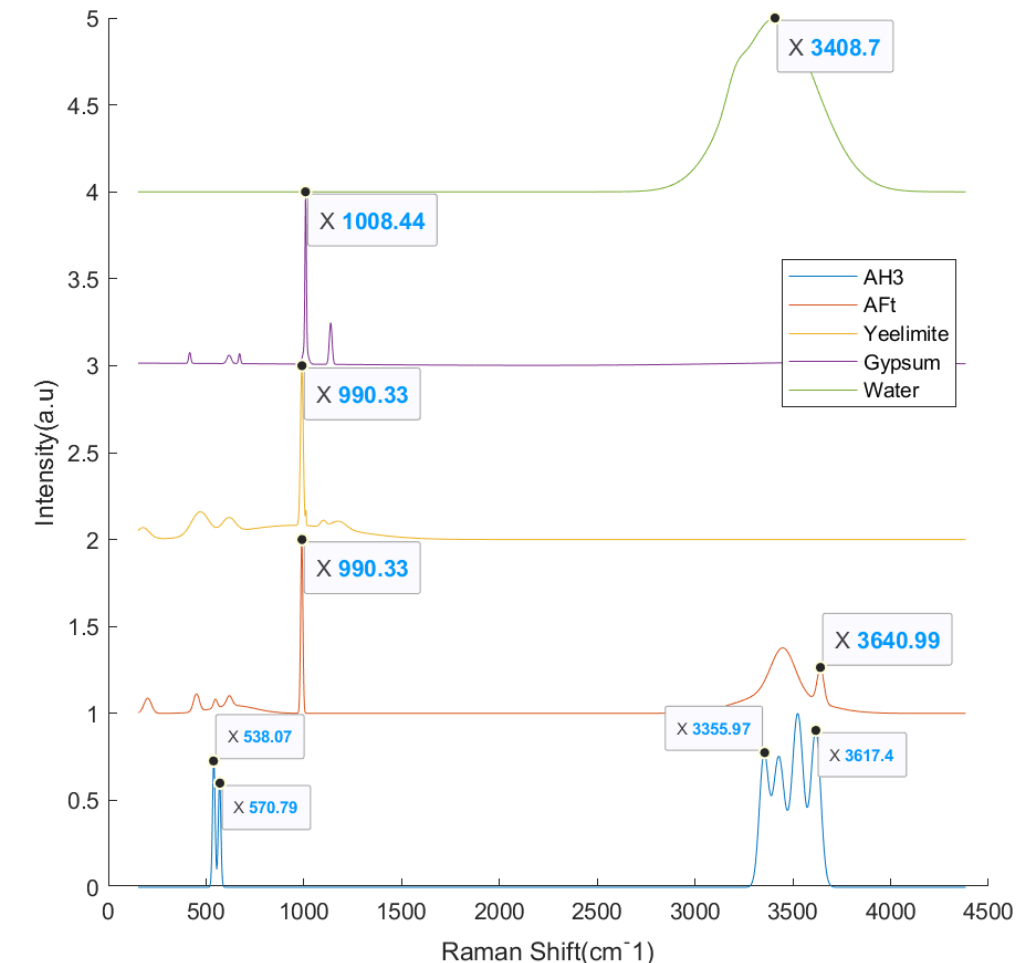
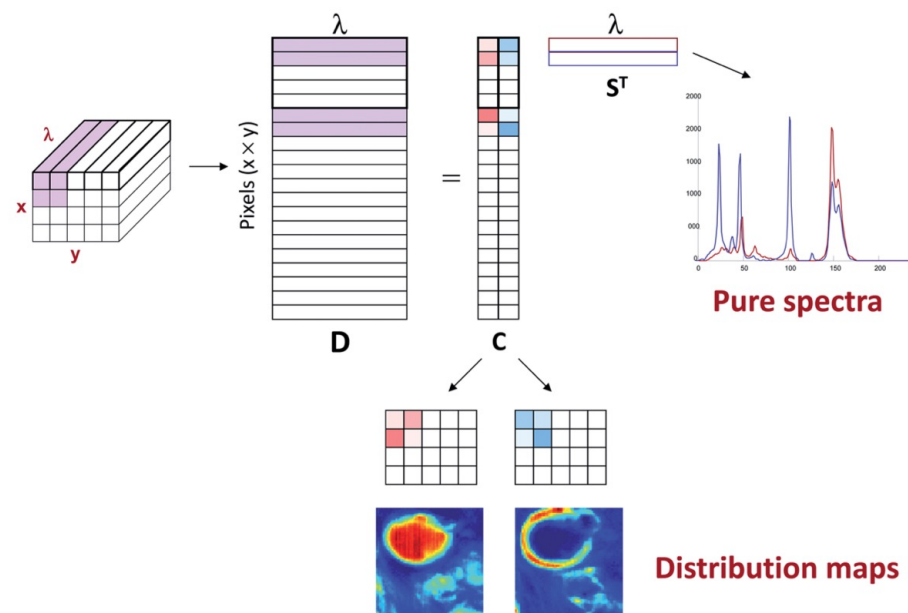


Figure. Basis spectra with Raman band assigned to specific vibrational mode (Lee., 2023).

# Examples for full-spectrum processing

- Multivariate curve resolution-alternating least squares (MCR-ALS)
  - MCR-ALS decomposes an experimental data matrix, D

$$\mathbf{D} = \mathbf{CS}^T + \mathbf{E}$$

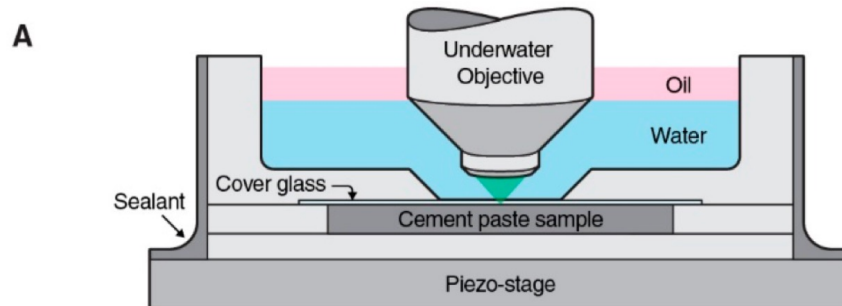


- $\mathbf{C}$  : concentration profile matrix
- $\mathbf{S}^T$  :resolved spectral matrix
- $\mathbf{E}$  : residual error matrix

Figure. MCR decomposition of a hyperspectral image data set (Juan et al., 2014).

# Quantitative analysis of the heterogeneous reaction of cementitious colloidal system using time-space-resolved characterization

- **Confocal Raman microspectroscopy (CRM) system**
    - High-resolution spectrometer
    - Automatic stage
    - Confocal microscope



$$\Delta_{lat} = \frac{0.61\lambda}{N.A.} = \frac{0.61 \cdot 532nm}{1.0} \sim 324nm$$

$$\Delta_{depth} = \pm \frac{4.4\lambda n}{2\pi(N. A.)^2} = \sim \pm 496 nm$$

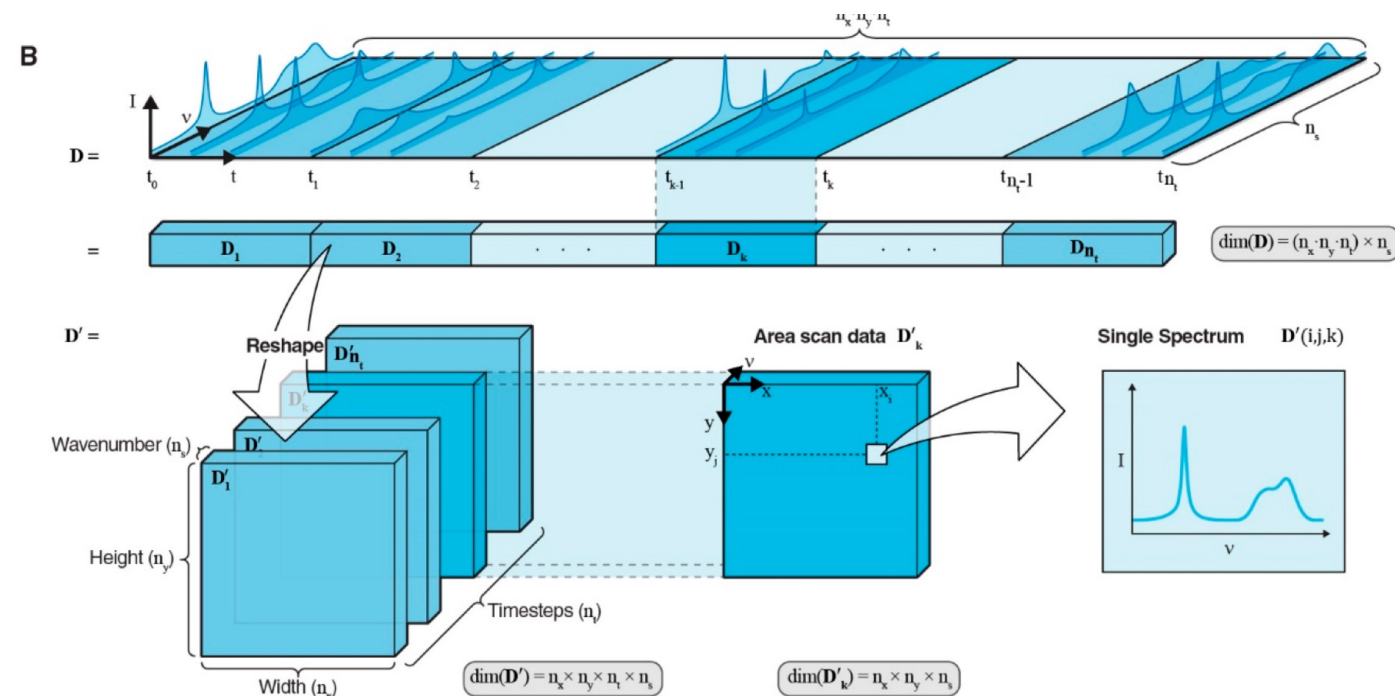


Figure. Schematics of the experimental setup and analysis procedures. (a) In situ underwater Raman experimental setup. (b) The raw hyperspectral Raman data D is partitioned with time and is reshaped to a 4D array (Loh et al., 2021)

# Quantitative analysis of the heterogeneous reaction of cementitious colloidal system using time-space-resolved characterization

- Basis analysis**

- Each entity of the matrix  $C_k$  is calculated by minimizing the error spectrum  $E$  in the following fitting

$$\underbrace{\mathbf{D}'(i, j, k)}_{1 \times n_s} = \underbrace{\mathbf{C}_k(i, j) \cdot \mathbf{B}}_{1 \times n_b} + \underbrace{\mathbf{E}(i, j, k)}_{n_b \times n_s}$$

- The principle of linear superposition**

- It works because Raman scattering cross-sections are very small
- The probability of a Raman scattered photon being lost because of another Raman scattering interaction is essentially zero

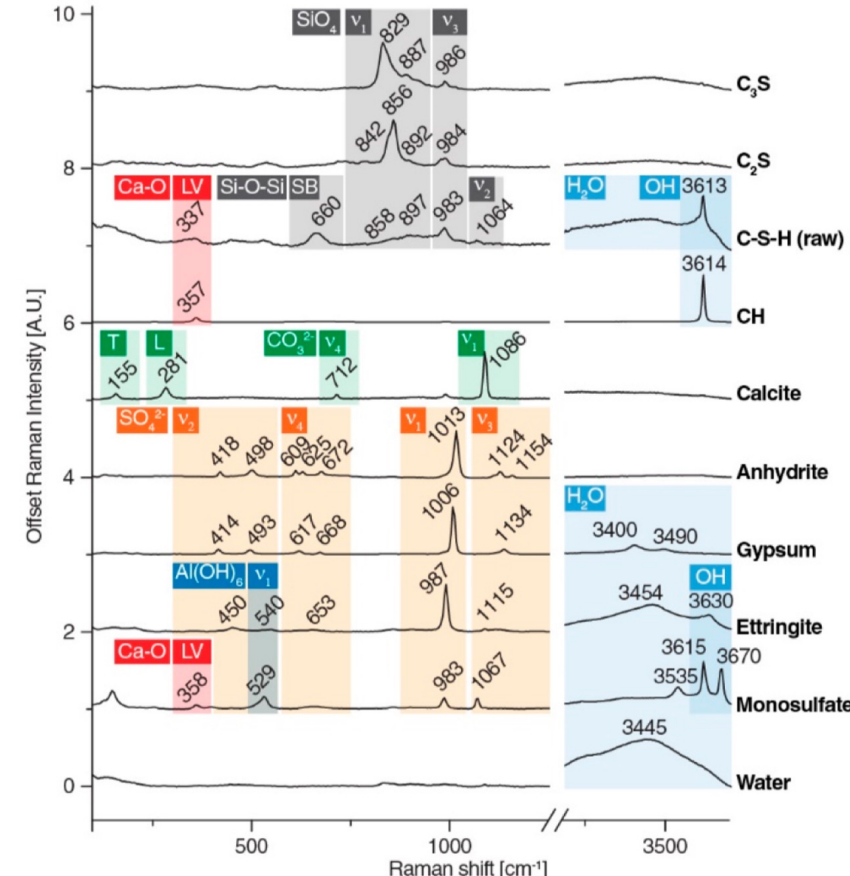


Figure. Basis spectrum with peak assignments. The peak position and vibrational modes are annotated..

# Quantitative analysis of the heterogeneous reaction of cementitious colloidal system using time-space-resolved characterization

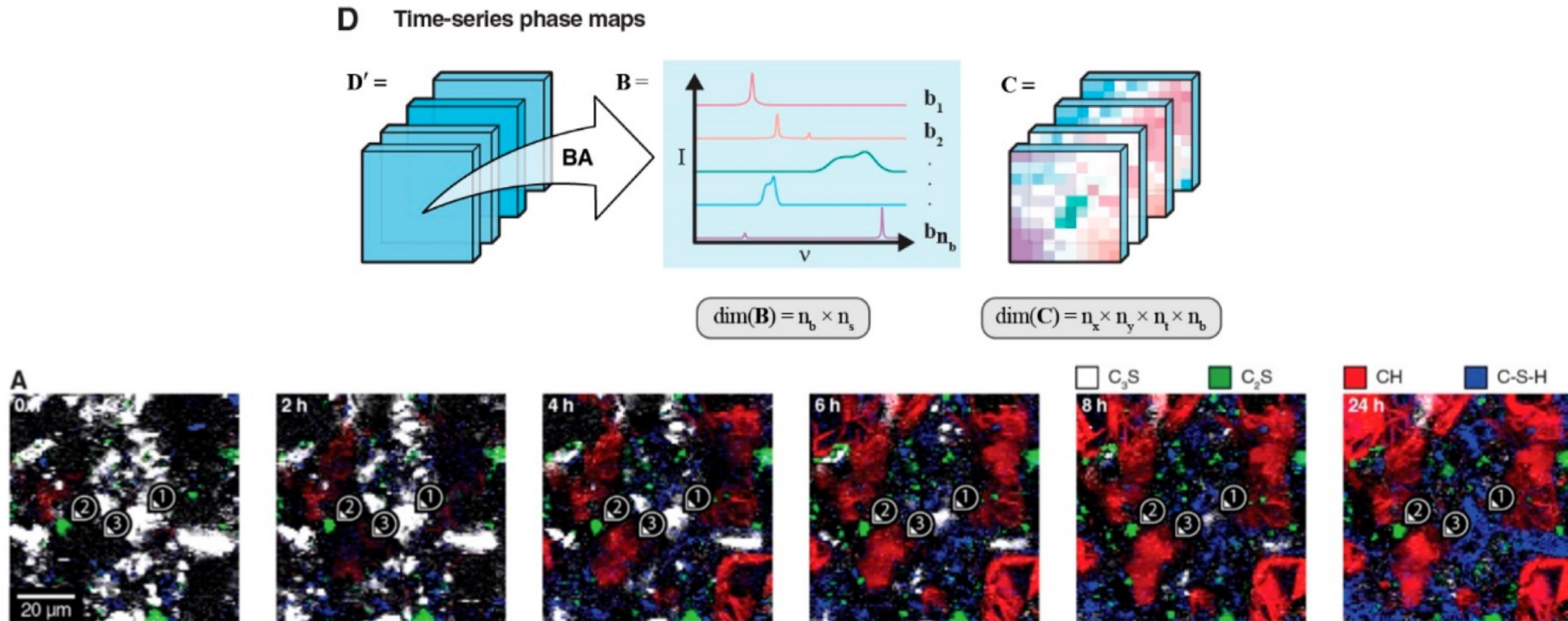
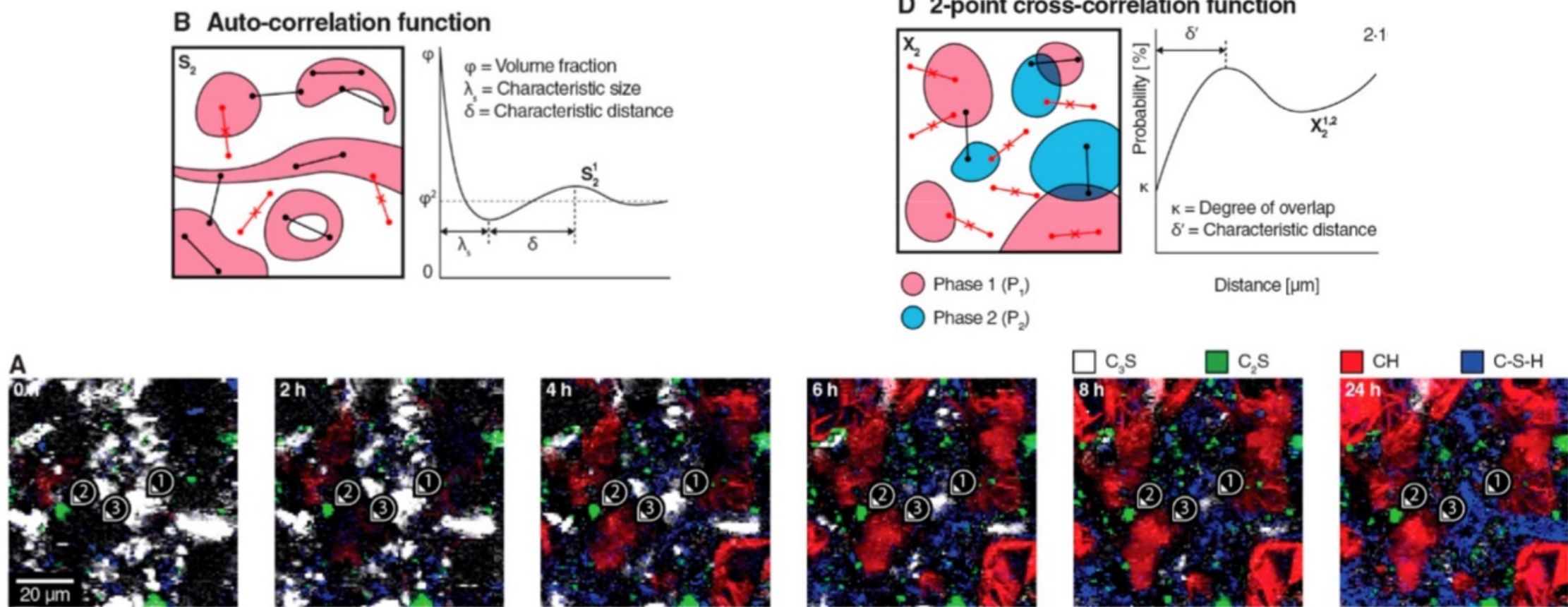


Figure. (d) The basis spectra  $B$  are generated with a basis analysis (BA). The phase maps  $C$  are visualized by overlaying the distribution of each basis spectrum. (a) Raman heatmaps of the main clinker phases and hydration products (Loh et al., 2021).

# Quantitative analysis of the heterogeneous reaction of cementitious colloidal system using time-space-resolved characterization



# Quantitative analysis of the heterogeneous reaction of cementitious colloidal system using time-space-resolved characterization

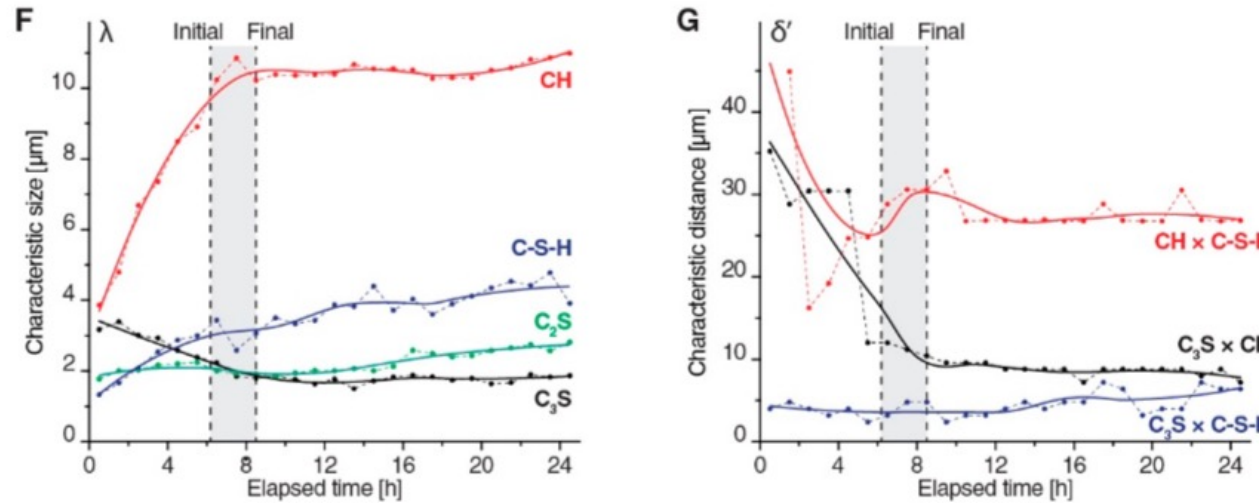


Figure. (f) The characteristic sizes of the phases are calculated from the autocorrelation graphs. (g) The characteristic distances between phases are calculated from the cross-correlation graphs.

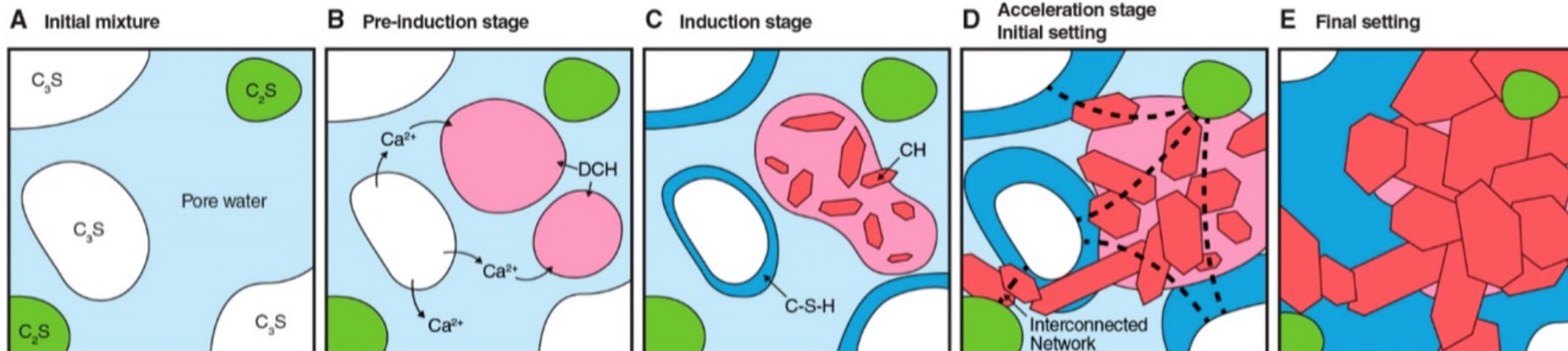


Figure. Schematic representation of early stage silicate hydration.

# Quantitative analysis of the content of carbon nanotubes in cement matrix using CRM system

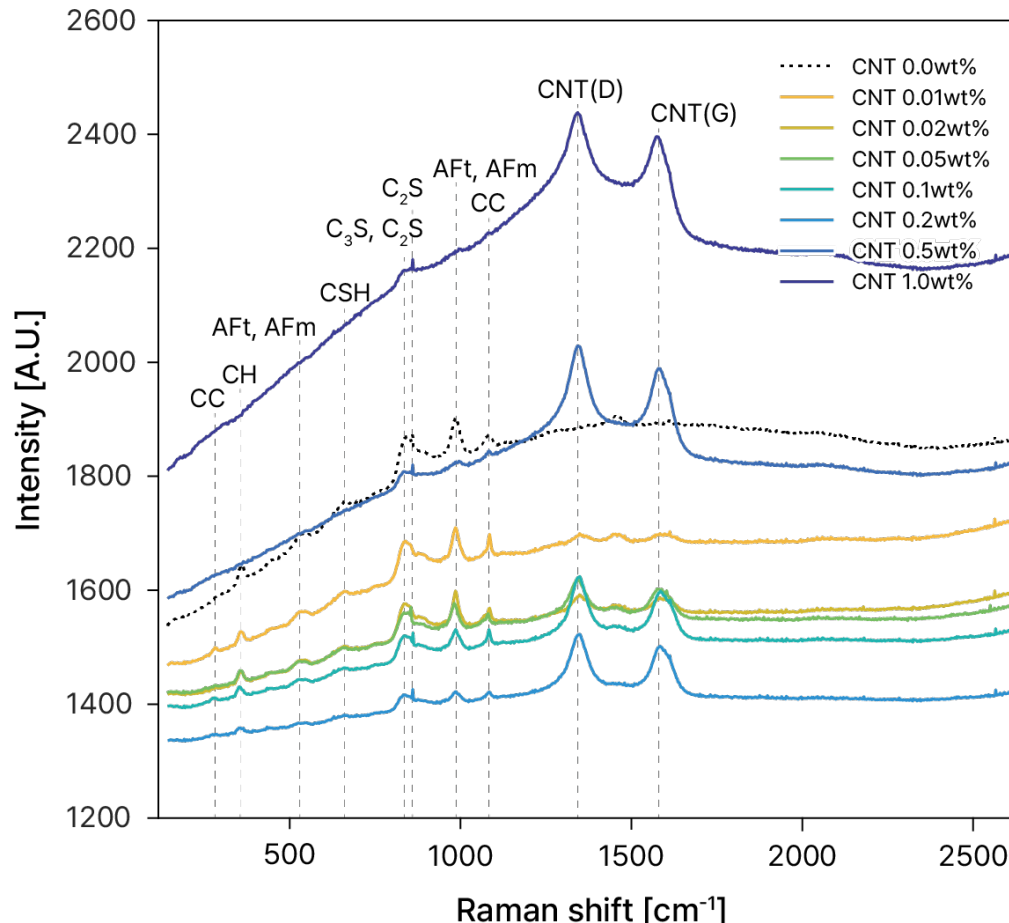


Figure. Average Raman spectra of specimens incorporating varying CNT concentrations.

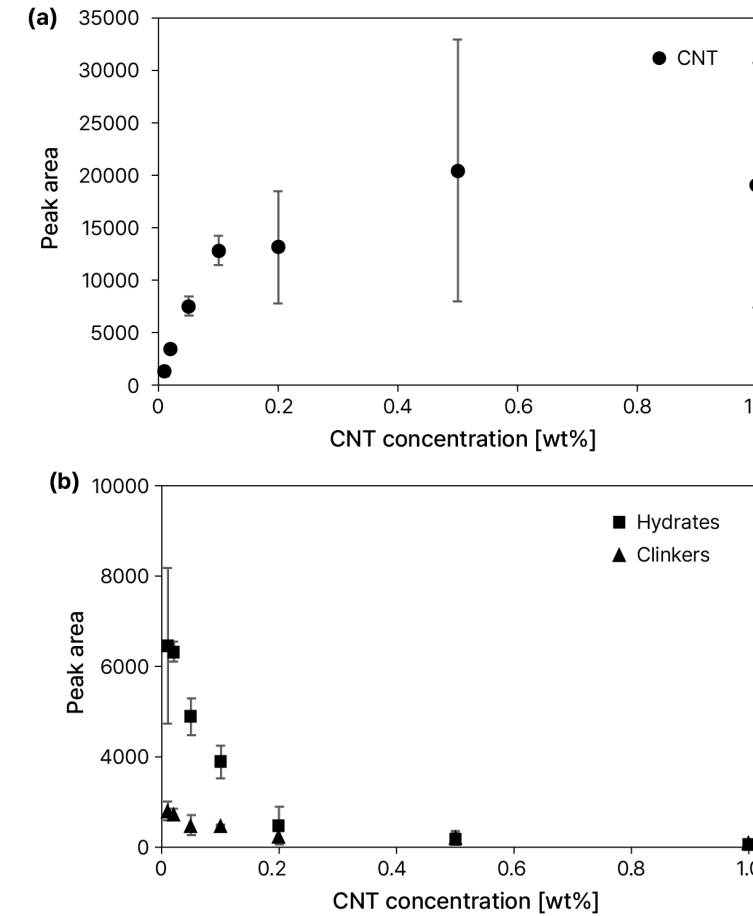


Figure. Peak areas of (a) the bands of CNT and (b) other phases (clinkers and hydrates) as a function of CNT concentration.<sup>35</sup>

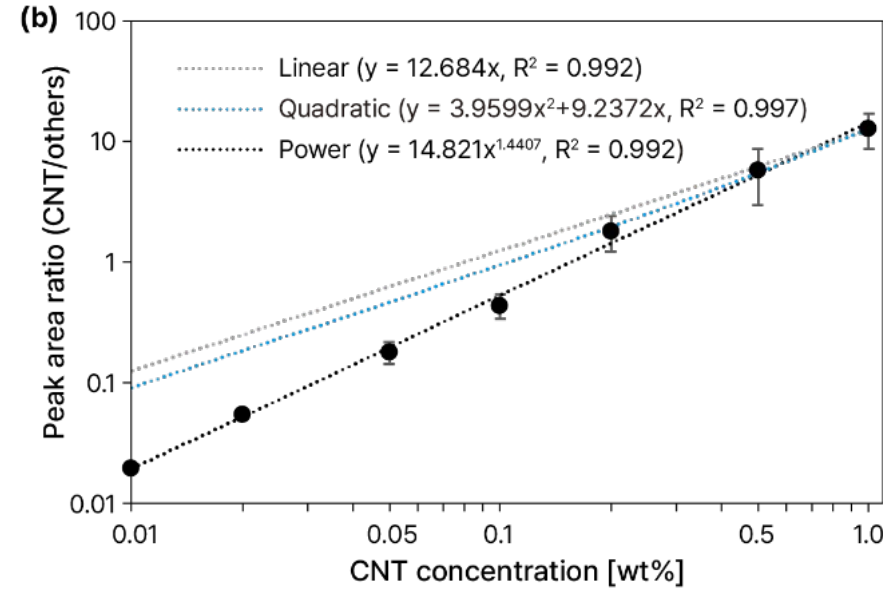
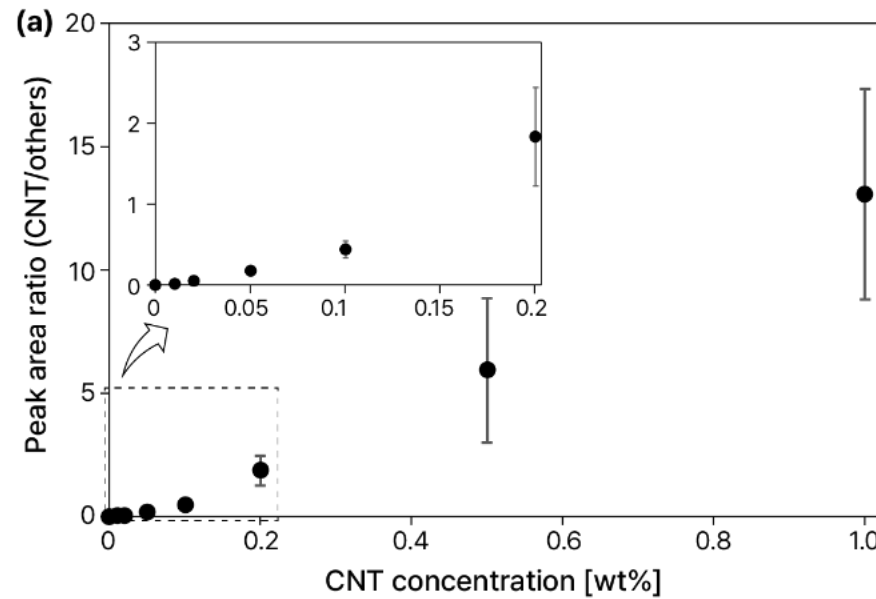


Figure. (a) Peak area of the bands of CNT as a function of CNT concentration. (b) Correlations between the peak area ratio (CNT/others) and CNT concentration of the CNT/cement composites plotted with a base-10 logarithmic scale on the x-, and y-axes.

Measured location	Peak area ratio	CNT concentration (wt%)
Bottom	0.0010	0.0013
Middle	0.0007	0.0010
Top	0.0018	0.0019
Mean (Standard deviation)		0.0014 (0.0005)
LD (Mean+3×standard deviation)		0.0028
LQ (Mean+10×standard deviation)		0.0062

# Precise determination of Mg/Fe ratios in olivine samples

## Olivine $[(\text{Mg}, \text{Fe})_2\text{SiO}_4]$

- an important mineral in geoscience
- commonly observed in widely varying lithologies
- Also found in ferronikel slag (FNS)

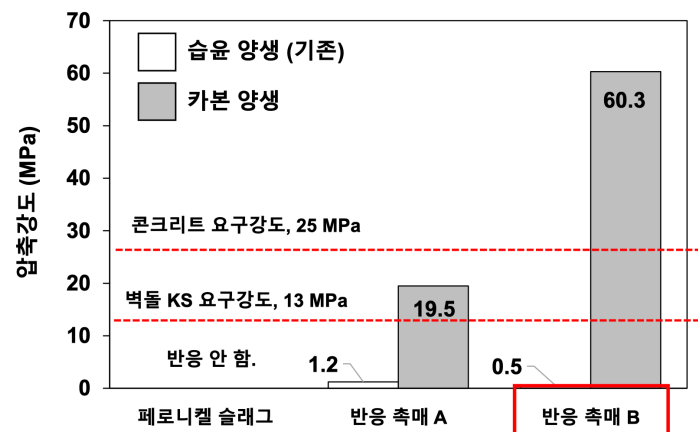


Figure. The compressive strength of cementless FNS binder with carbon curing with addition of catalyst (Jeon, 2023).

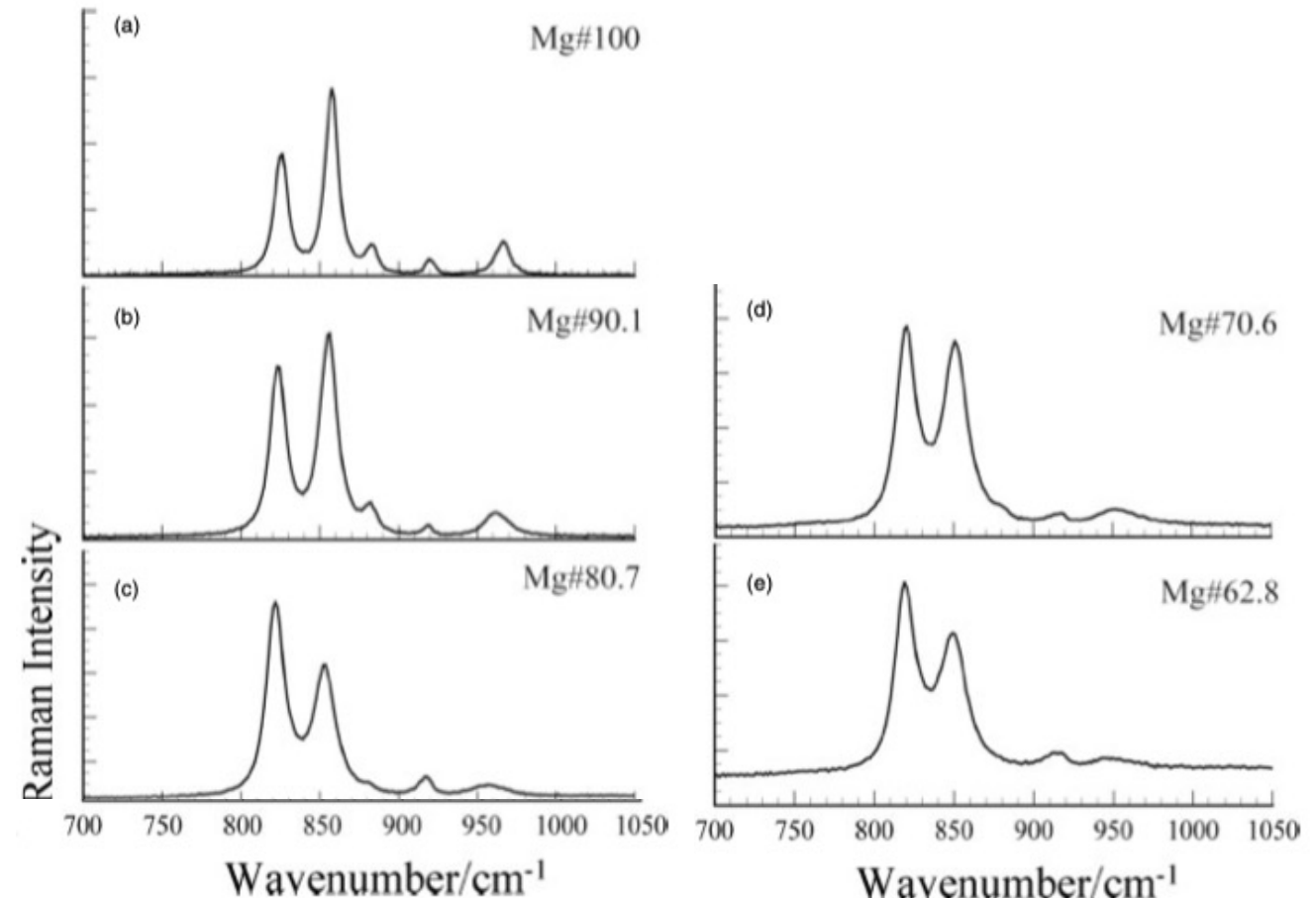


Figure. Raman spectrum in the 700–1050 cm<sup>-1</sup> region for Mg# of 100 (a), 90.1 (b), 80.7 (c), 70.6 (d), and 62.8 (e).

# Precise determination of Mg/Fe ratios in olivine samples

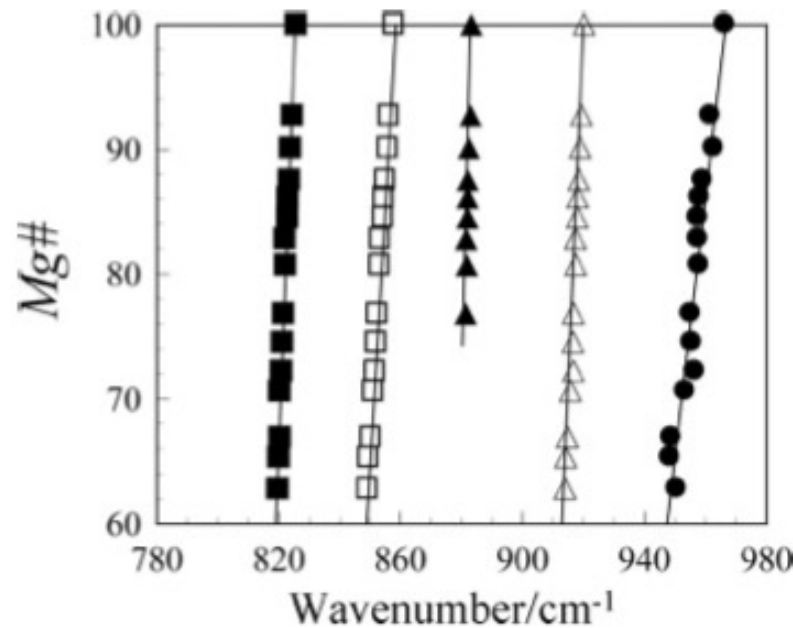


Figure. Relations between Raman peak wavenumbers and Mg# for the five peaks.

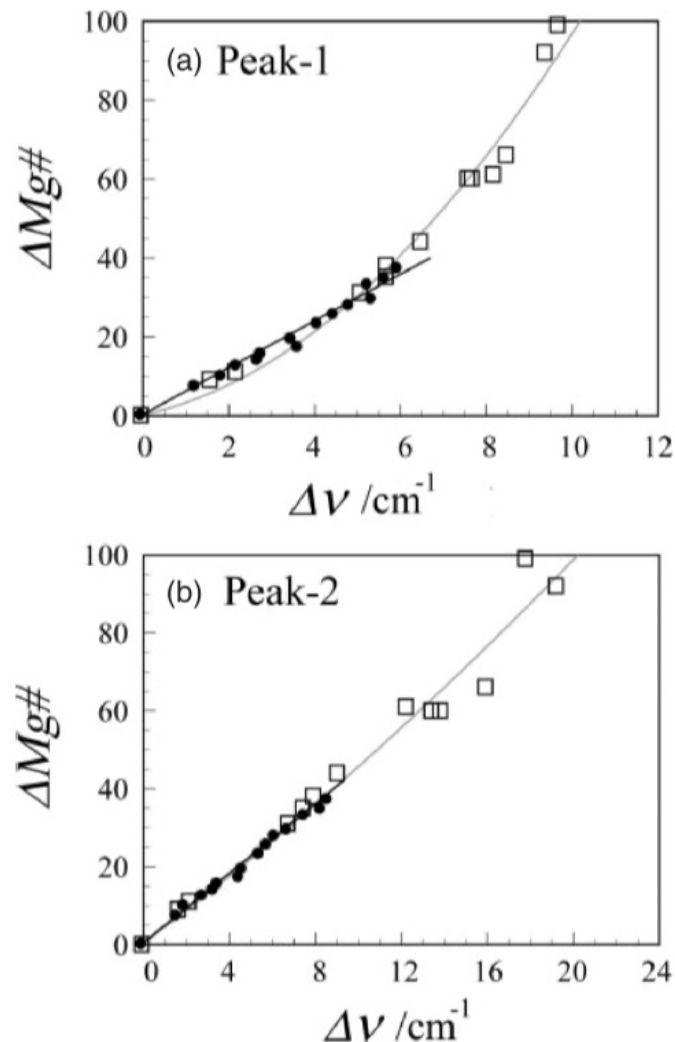
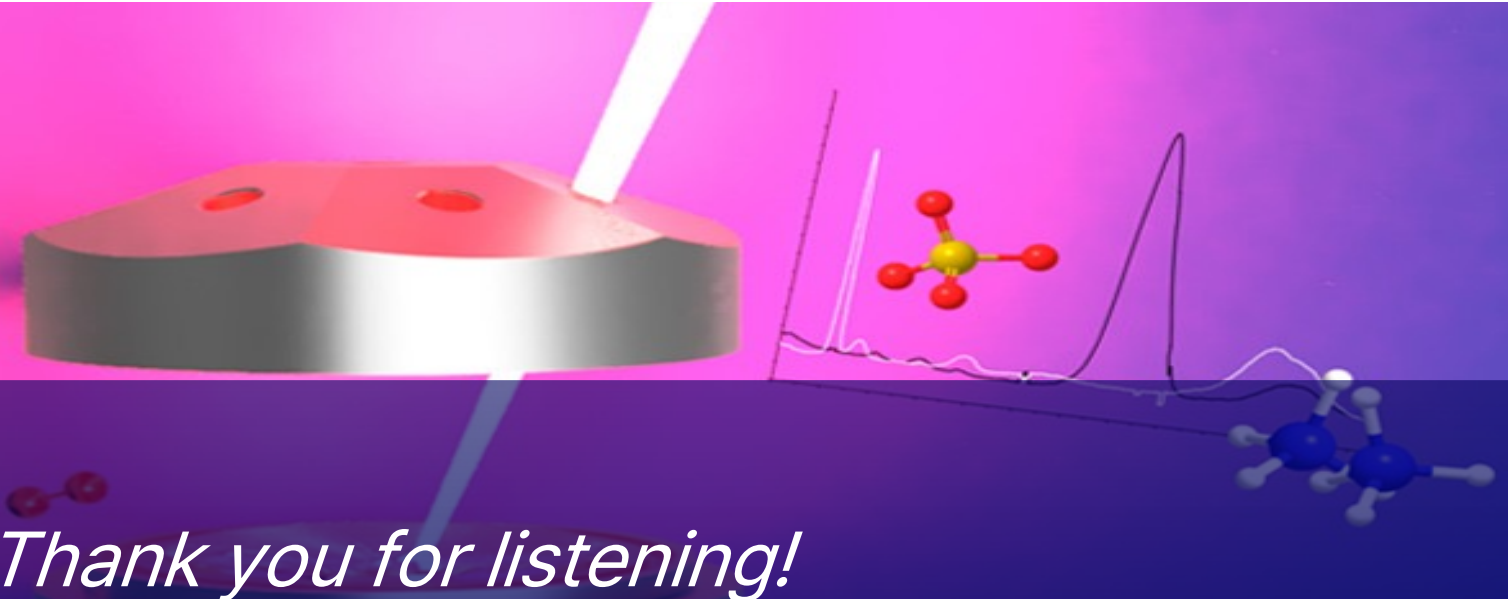


Figure.  $\Delta \text{Mg}\#$  versus  $\Delta v$   
(a) for peak 1 and  
(b) for peak 2.

# Conclusion

- Raman spectroscopy coupled with confocal microscope is powerful tool for time-spatial resolved analysis of heterogeneous material.
- The footprint of molecule, crystal, even amorphous phases can be identified if it is Raman-active.
- Quantitative analysis can be done by constructing the calibration curve with reference samples by using properly normalized peak area or the shifts in peak position.
- For robust and reliable results, preprocessing of spectra is necessary but care must be taken not to eliminate important information and not to distort the signal.



*Thank you for listening!*

# Exploring Building Materials with Raman Spectroscopy:

## A Beginner's Journey through Research Progress and Discoveries



Presented by Jiseul Park  
Postdoctoral Researcher



**Multiscale Structural Materials Lab.**  
Advanced Technology in Structural Materials